

Formation of Spanning Water Networks on Protein Surfaces via 2D Percolation Transition

Alla Oleinikova, Nikolai Smolin, Ivan Brovchenko,* Alfons Geiger, and Roland Winter

Physikalische Chemie, Universität Dortmund, Otto-Hahn-Str. 6, Dortmund, D-44221, Germany

Received: September 10, 2004; In Final Form: November 18, 2004

The formation of spanning hydrogen-bonded water networks on protein surfaces by a percolation transition is closely connected with the onset of their biological activity. To analyze the structure of the hydration water at this important threshold, we performed the first computer simulation study of the percolation transition of water in a model protein powder and on the surface of a single protein molecule. The formation of an infinite water network in the protein powder occurs as a 2D percolation transition at a critical hydration level, which is close to the values observed experimentally. The formation of a spanning 2D water network on a single rigid protein molecule can be described by adapting the cluster analysis of conventional percolation studies to the characterization of the connectivity of the hydration water on the surface of finite objects. Strong fluctuations of the surface water network are observed close to the percolation threshold. Our simulations also furnish a microscopic picture for understanding the specific values of the experimentally observed hydration levels, where different steps of increasing mobility in the hydrated powder are observed.

Introduction

Water adjacent to the protein surface (so-called “hydration”, “bound”, or “biological” water) strongly influences the structural and dynamical properties of proteins and enables their function.^{1–3} With increasing hydration level below monolayer coverage, a hydrogen-bonded water network which fully spans the protein surfaces appears.^{2,4–13} Experimental studies on protein powders indicate that, with the appearance of a system-spanning water network via a 2D percolation transition, onset of some biological function of proteins is observed.^{4–7,13} The relation between these two phenomena is not clear yet. Computer simulations can help to clarify this problem by studying the behavior of various molecular properties at the percolation threshold.

One may assume that the appearance of protein function is enabled by a 2D water network, spanning over a single protein molecule. In this case, protein function could be related to some specific changes of protein structure and dynamics or to the charge transfer between its various functional groups. Such an approach is widely used in theoretical and computer simulation studies of hydrated proteins (for example, the study of protonic conductivity at protein surfaces¹⁴ and the glass transition of hydrated proteins¹⁵). Many properties of single hydrated protein molecules have been studied in detail by computer simulations. However, relating the obtained results to the properties of real protein systems is not trivial. On the other hand, in powder protein, molecules form complex extended protein surfaces, and a water network which spans such a “collective” surface may cover each protein molecule only partially. Simulation studies of hydrated protein powders could be more directly related to the available experiments.^{2,4–13} However, studies of the structural and dynamic properties of such systems are hampered by several problems. The structure of a protein powder as well as its changes with hydration level is unknown. Additionally, the conformation of the protein molecules could change upon hydration. Finally, any realistic simulation of a protein powder

needs an essential number of protein molecules and a variation of their arrangement. With these ramifications in mind, we start approaching this problem by considering a single rigid protein molecule and two simple molecular arrangements at various hydration levels.

To understand the onset of protein function, the structural and dynamical properties of hydrated proteins should be studied below and above the percolation threshold of hydration water. Our simulations furnish information about the location of the percolation threshold, the water distribution at protein surfaces close to the percolation transition, and particular properties of spanning and nonspanning water networks.

Although, some properties of bound water at the surface of single protein molecules at low hydration levels were studied by computer simulations (see, for example, refs 16–18), the formation of a spanning water network via a percolation transition was studied neither for single proteins nor for protein powders. In this paper, we present the first computer simulation study of this phenomenon, using a single rigid lysozyme molecule and two model powders of lysozyme. The simplified powder models do not take into account possible changes of the powder structure and lysozyme conformation with hydration level, but allow us to explore the hydration in a wide range, including the percolation threshold. We analyze the clustering of water molecules on the protein surface at various hydration levels and two temperatures (300 and 400 K). The higher temperature was considered to explore the temperature effect on water clustering and to avoid a possible 2D condensation of water (layering transition), which in general could be expected at hydrophilic surfaces at lower temperatures.¹⁹ The percolation transitions in the lysozyme powders were located by analyzing the water clustering at various hydration levels, using the conventional methods, which are applicable to infinite systems.²⁰ To develop an appropriate method to study the formation of a spanning network in finite, closed systems, such as the surface of a single protein, we studied additionally the clustering of water on the surface of hydrophilic spheres of several sizes.

* Author to whom correspondence should be addressed. E-mail: brov@heineken.chemie.uni-dortmund.de.

This method was then applied to locate the percolation transition of water at the surface of a single lysozyme molecule.

Methods

Hen egg white lysozyme²¹ is a small globular protein with 129 amino acid residues and contains α -helices and a triple-stranded β -sheet in two structural domains. Lysozyme molecule (molecular mass of about 14.5 kDa) was modeled, using the crystallographic heavy atom coordinates from the Protein Data Bank²² (entry 2LYM²³) and AMBER force-field from ref 24, which treats all atoms, including hydrogens, explicitly. The TIP4P model²⁵ was used for water.

Molecular dynamics (MD) simulations of the lysozyme + water systems were done in the *NVT* ensemble. The temperature was kept constant by a Berendsen thermostat²⁶ with a coupling time of 0.5 ps. A spherical cutoff at 9 Å was used for the van der Waals interactions, and the particle mesh Ewald²⁷ summation method was used for the calculation of the electrostatic interactions. Integration time steps of 2 and 1 fs were used at $T = 300$ and 400 K, respectively. For the residues we chose the charge states corresponding to pH 7. The total charge of +8e on the protein surface was then neutralized by a uniform distribution of the opposite charge between all protein atoms in order to make the system neutral (adding a charge of $-8e/1960 \approx -0.004e$ to each atom of the lysozyme molecule). To remove bad contacts and to adapt our system to the force field, energy minimization was carried out with Steepest Descent and Conjugate Gradient methods.

The rigid model lysozyme molecule was fixed in the center of a cubic box (edge length 60 Å), and periodic boundary conditions were applied. N_w water molecules were then randomly placed in the free space of the simulation box to provide the chosen hydration level. The water molecules were equilibrated at constant temperature during 1.5 to 3.0 ns in the field of the protein atoms. The number of water molecules varied from $N_w = 200$ to 600 at $T = 300$ K and from 400 to 800 at $T = 400$ K. Subsequently, the water clustering was analyzed every hundredth integration step (every 0.2 and 0.1 ps at $T = 300$ and 400 K, respectively), and trajectories from 8 to 15 ns were used for these purposes.

The structure of an amorphous lysozyme powder, used for the experimental studies, is not available. In low-humidity tetragonal crystals²⁸ with a partial density of lysozyme of about $\rho \approx 0.80$ g cm⁻³, approximately 120 water molecules are in the first hydration shell of lysozyme molecules. To explore a wide range of hydration levels up to monolayer coverage (about 300¹² to 420²⁹ water molecules), the partial density of lysozyme in the powder should be <0.80 g cm⁻³. Therefore, we studied an amorphous model protein powder with a dry protein density of $\rho = 0.66$ g cm⁻³ (densely packed model powder). It was prepared by placing six rigid lysozyme molecules randomly in a cubic box (edge length 70 Å) without close intermolecular contacts (less than 3.5 Å) between any atoms. Then, during a low-temperature simulation in the *NPT* ensemble ($T = 10$ K, $P = 1$ bar), the length of the simulation box shrank to about 60 Å and the above given density of the dry powder was obtained.

To explore the effect of protein packing on the water percolation transition, we also simulated an artificial loosely packed powder with a density of the dry protein of $\rho = 0.44$ g cm⁻³. This model powder contained four lysozyme molecules randomly arranged in a cubic box (edge length 60 Å) without close contacts, but each lysozyme molecule had at least one medium-ranged contact with another neighbor in the box (shortest intermolecular distance between 3.5 and 5 Å).

The resulting configurations of the model lysozyme powders with various numbers N_w of water molecules added were used as starting points for subsequent MD runs with periodic boundary conditions in all directions. In the densely packed powder, N_w varied from 500 to 1200 at $T = 300$ K and from 700 to 1200 at $T = 400$ K. In the loosely packed powder, N_w varied from 800 to 1400 at $T = 300$ K. Integration steps of 2 fs were used for all simulations of the powder. After initial equilibration for 1 to 3 ns, water clustering was analyzed every hundredth integration step during runs of 12 to 14 ns.

Water clustering and percolation on the surfaces of structureless hydrophilic spheres with radii $R_{sp} = 15, 30,$ and 50 Å were also investigated by Monte Carlo (MC) simulations in the *NVT* ensemble. The water–surface interaction was described in this case by a (9–3) Lennard-Jones potential between the water oxygen and the surface with $\sigma = 2.5$ Å and a well-depth $U_0 = -4.62$ kcal/mol. To avoid 2D condensation, simulations were performed at $T = 425$ K, exceeding the critical temperature of the layering transition ($T \approx 400$ K) for this water–surface interaction.¹⁹ To explore the temperature effect, clustering at the surface of the smallest sphere was also studied at $T = 475$ K. Various hydration levels of the hydrophilic spheres were obtained by placing different numbers N_w of water molecules in the simulation box. N_w varies from 150 to 450 for the sphere of radius $R_{sp} = 15$ Å, from 900 to 1300 for $R_{sp} = 30$ Å, and from 2500 to 3400 for $R_{sp} = 50$ Å. Configurations after every 1000 MC steps were analyzed; that provides up to 5×10^5 analyzed configurations for each hydration level.

The number of water molecules in the first hydration shell of the lysozyme molecule was calculated by counting up to the minima in the pair correlation functions between the water oxygen and the heavy atoms of the protein. A water molecule belongs to the first hydration shell, when the shortest distance between its oxygen and the nearest heavy atom of the protein is <3.5 Å for N, O, or S atoms or <4.5 Å for C atoms.³⁰ Similarly, in the case of the hydrophilic spheres, a water molecule was attributed to the first hydration shell when the distance from its oxygen to the surface is less than 4.5 Å.¹⁹

Water molecules belong to the same cluster if they are connected by a continuous path of hydrogen-bonds.^{31–33} Two water molecules were considered as hydrogen-bonded when the distance between the oxygen atoms is <3.5 Å and the water–water interaction energy is <-2.4 kcal/mol. The occurrence frequency of water clusters of various sizes S is described by the cluster size distribution n_S , which at the percolation threshold obeys a power law $n_S \sim S^{-\tau}$ with critical exponent $\tau = 187/91 \approx 2.05$ and $\tau \approx 2.2$ in the case of 2D and 3D percolation, respectively.²⁰ The mean cluster size $S_{\text{mean}} = \sum n_S S^2 / \sum n_S S$, calculated excluding the largest cluster, diverges at the percolation threshold in an infinite system or passes through a maximum when approaching the threshold in a finite system. The fractal dimension d_f of the largest cluster at the percolation threshold is lower than the Euclidean dimension of the system; in the 2D case it can be expressed as $d_f^{2D} = 91/48 \approx 1.896$,²⁰ whereas $d_f^{3D} \approx 2.53$ in 3D systems.³⁴ We evaluated d_f from the function $m(r)$, which describes how the mass distribution of the largest cluster scales with distance r :

$$m(r) \sim r^{d_f} \quad (1)$$

We used these cluster properties to study the percolation transition in all model systems. In the protein powders, we also calculated the spanning probability R to find in the periodic system an infinite cluster which spans (“wraps”) the simulation box at least in one direction. The value of R at the *true*

percolation threshold does not depend on the system size, but it is sensitive to the used spanning rule and to the system dimensionality. For the rule used in the present paper (spanning the cell with periodic boundaries, sometimes also called “wrapping” the system, either in x , y , or z direction), the values of R at the true percolation threshold given in the literature for simple 2D and 3D lattices range from about 0.5 to almost 1.^{35–38}

The hydration level of the powders can be described not only by the number of inserted water molecules N_w , but also by C , the water mass fraction, and by the ratio h of the water mass to the mass of the dry protein, which is widely used in the studies of protein hydration. In the case of the single protein or the hydrophilic sphere, the hydration level was characterized also by the surface coverage C^* . For a spherical surface, $C^* = N_w / 4\pi(R_{sp} + r_0)^2$, where r_0 is the distance from the surface to the first maximum of the oxygen local density (r_0 is about 3 Å for the considered hydrophilic surface¹⁹). To estimate the surface coverage of the single lysozyme, its solvent-accessible surface area (SASA) was used, that is, $C^* = N_w / \text{SASA}$. A probe sphere of a radius of 1.4 Å yields an estimation of the SASA for our model lysozyme of about 6900 Å².

Conventional percolation analysis does not apply definite numerical criteria to estimate the accuracy of the probability distributions, such as R , n_s , $m(r)$, and so forth. Normally, visual inspection of the obtained probability distributions and the observation that longer simulations do not change them noticeably are considered to be sufficient to make reliable conclusions. In the present studies, we additionally calculated at the i th simulation step the running average value y_i^{av} of a given probability function y_i by averaging over all previous configurations: $y_i^{\text{av}} = [y_{i-1}^{\text{av}}(i-1) + y_i] / i$. In all samples studied, the number of the analyzed configurations provided sufficient sampling: the running average values y_i^{av} did not show any monotonic trend and varied within only 1% during the last 10⁴ simulated configurations.

Results

2D Percolation Transition of Water in Lysozyme Powders.

Some properties of the water clusters in our model of densely packed lysozyme powder at $T = 300$ and 400 K are shown in Figure 1 as a function of the water mass fraction C . In infinite systems, R changes sharply at the percolation threshold from 0 to 1. In finite systems, the percolation threshold is smeared out and a gradual increase of R is observed in some range of hydration (Figure 1, upper panel). Taking into account studies of percolation in various lattice and continuous models,^{35–38} we defined the water concentration $C_1(R)$, where the probability R reaches about 50%, as a lowest boundary of the percolation threshold. We obtained the values $C_1(R) = 0.122 \pm 0.002$ at $T = 300$ K and $C_1(R) = 0.149 \pm 0.002$ at $T = 400$ K, shown in Figure 1 by blue vertical lines. The mean cluster size S_{mean} shows a broad maximum close to the hydration level $C_1(R)$ for both temperatures (Figure 1, middle panel). The mean cluster size S_{mean} in finite systems passes a maximum below the percolation threshold.²⁰ This supports the attribution of the concentration $C_1(R)$ to the lowest limit for the percolation threshold.

The existence of a permanent spanning cluster corresponds to $R = 1$. If we attribute for our finite powder systems the appearance of a permanent spanning cluster to $R = 0.99$, this corresponds to concentrations $C_2(R) = 0.159$ at $T = 300$ K and to $C_2(R) = 0.181$ at $T = 400$ K (green vertical lines in Figure 1). These concentrations could serve as estimates of the upper boundary for the percolation threshold, as the true percolation threshold is reached at $R < 0.99$ independent from system size and dimensionality.^{35–38}

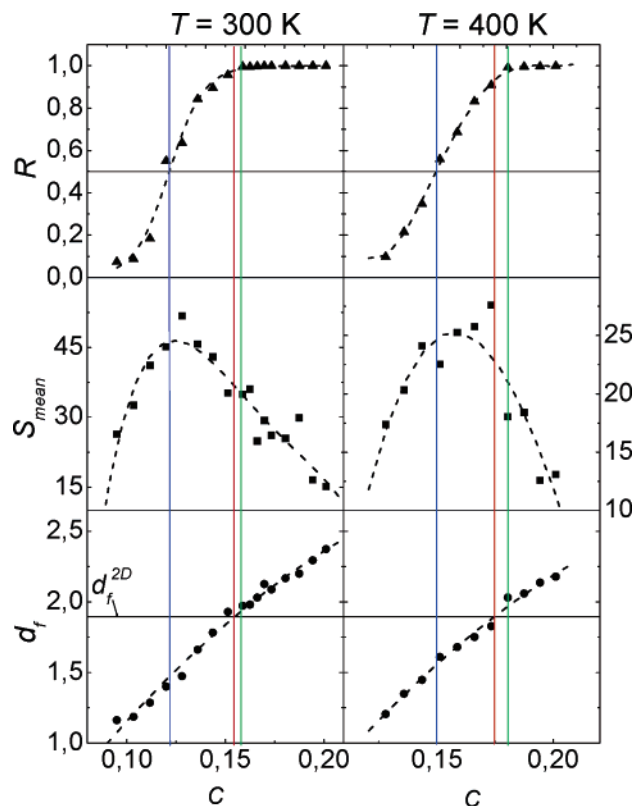


Figure 1. 2D percolation transition of water in the hydrated densely packed powder of lysozyme at $T = 300$ K (left panel) and 400 K (right panel). Spanning probability R (triangles, upper panel), mean cluster size S_{mean} (squares, middle panel), and fractal dimension of the largest cluster d_f (circles, lower panel) are shown as a function of the mass fraction C of water. The dashed lines are guides for the eyes. Vertical lines indicate the water fractions $C_1(R)$ (blue), $C_2(R)$ (green), and $C_2(d_f)$ (red).

To determine the dimensionality of the observed percolation transition, we examined the fractal dimension of the largest cluster. For this purpose, the function $m(r)$, which describes the mass distribution within the largest cluster, averaged over all molecules of this cluster as reference site, was calculated. Typical distributions $m(r)$ at different hydration levels of densely packed lysozyme powder are shown in Figure 2 (upper panel). Fits of $m(r)$ to the power law (eq 1) are shown as dashed red lines. The effective values of d_f , found from the fits, are shown in Figure 2 (uncertainties in brackets correspond to the confidence level 95%).

Below the percolation threshold, the largest cluster is not a fractal object and $m(r)$ does not follow a power law behavior, which can be clearly seen in a double logarithmic scale (see Figure 2, lowest curve). The obtained values of d_f are essentially effective in this case. Approaching the percolation threshold, the largest cluster evolves to a fractal object. Indeed, a behavior of $m(r)$ at $T = 300$ K close to a power law is observed in the range of $r > 10$ Å (see middle and upper curves in Figure 2). At the hydration level $C = 0.144$ ($N_w = 800$, Figure 2, middle curve), the effective value $d_f = 1.782$ is slightly lower than $d_f^{2D} = 1.896$ (green lines), which is observed at the 2D percolation threshold of water on an unstructured planar hydrophilic surface with periodic boundaries³⁹ (blue squares). The deviation of $m(r)$ downward from the power law behavior at $r < 10$ Å, observed at various hydration levels (Figure 2, lower panel), could reflect the structured character of the lysozyme surface.

The effective fractal dimension d_f obtained gradually increases with the hydration level (see Figure 1, lower panel). In the

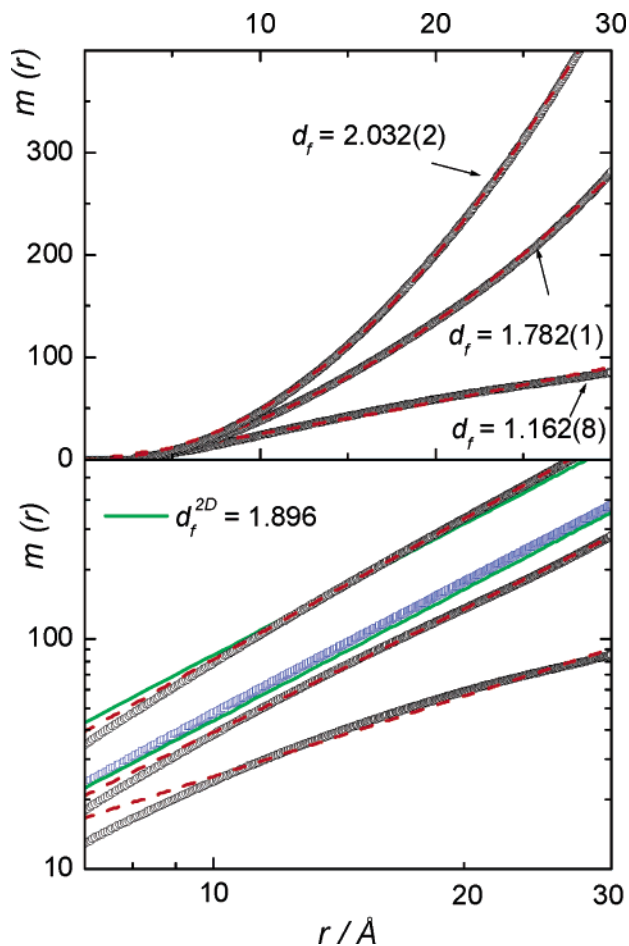


Figure 2. Determination of the fractal dimension d_f of the largest water cluster at $T = 300$ K in the densely packed powder. $m(r)$ vs r (black circles) and their fits to eq 1 (red dashed lines) are shown in a linear scale (upper panel) and in a double logarithmic scale (lower panel). The hydration level increases from bottom to top: $N_w = 500, 800,$ and 950 . $m(r)$ for the largest water cluster at an unstructured planar hydrophilic surface at the percolation threshold is shown by blue squares. This data set and data for $N_w = 950$ are shifted vertically in the lower panel.

hydration range, where the true percolation threshold is expected (between $C_1(R)$ and $C_2(R)$), d_f varies from about 1.5 to about 1.95 for both temperatures. This evidences the 2D character of the observed percolation transition of water in densely packed lysozyme powder. The fractal dimension of the largest cluster achieves the value d_f^{2D} at water mass fractions $C_2(d_f) = 0.155 \pm 0.002$ and 0.175 ± 0.002 at $T = 300$ and 400 K, respectively, that is, very close to the corresponding values of $C_2(R)$. Note, that with further increase of the hydration level, the fractal dimension d_f increases toward the value $d_f^{3D} \approx 2.53$ of 3D percolation,³⁴ in agreement with experimental observations.⁵ The difference between the mass fractions of water, corresponding to the estimated lower and upper boundaries for the true percolation threshold in densely packed powder, is only about 0.03 and slightly decreases with increasing temperature.

A similar relation between R , S_{mean} , and d_f was observed in simulation studies of the water percolation on a planar hydrophilic surface.³⁹ It was shown that the difference between $C_1(R)$ and $C_2(R)$, caused by the finite size of the simulated system, vanishes with increasing system size in a way that the value $C_1(R)$ approaches $C_2(R)$.³⁹ The hydration level $C_2(d_f)$ of water in finite systems was found to be not very sensitive to the system size. Therefore, the values of $C_2(d_f)$, given in Table 1, could be reasonable estimates of the true 2D percolation threshold in the

TABLE 1: Location of the Percolation Transition of Water in Lysozyme Powders, Determined on the Basis of the Fractal Dimension of the Largest Cluster^a

system	T (K)	$C_2(d_f)$	h	N_w/N_p	n_H
densely packed	300	0.155 ± 0.003	0.183 ± 0.003	146 ± 3	2.30
densely packed	400	0.175 ± 0.002	0.212 ± 0.003	169 ± 2	2.02
loosely packed	300	0.262 ± 0.002	0.355 ± 0.003	282 ± 2	1.94

^a The threshold hydration level, when d_f achieves the 2D value $d_f^{2D} = 1.896$, is given in various terms: water mass fraction $C_2(d_f)$, level of hydration h in grams of water per gram of dry protein, and number of water molecules per lysozyme N_w/N_p . n_H is the average number of water–water hydrogen-bonds at the threshold.

considered densely packed lysozyme powder. Note also that the average number n_H of water–water hydrogen-bonds, which are formed by each water molecule, is about 2.32 and 2.04 at the mass fraction $C_2(d_f)$ (Table 1) at $T = 300$ and 400 K, respectively. These values are close to the percolation threshold values in 2D lattices.²⁰ In the particular case of a square lattice (the most relevant case for a dense water monolayer⁴⁰), the threshold numbers of bonds are 2.00 and 2.37 for bond and site percolation, respectively.²⁰ The decrease of the threshold value n_H with temperature could be attributed to the trend toward three-dimensionality as a result of weaker localization of the water molecules at the surface at higher temperatures. (The threshold number of bonds in 3D systems is always lower than in 2D systems.²⁰) This agrees with the threshold value n_H (≈ 1.8) obtained for quasi-2D water percolation in an aqueous solution of tetrahydrofuran.³²

Cluster size distributions n_S of water in densely packed lysozyme powder at $T = 400$ K at different hydration levels are shown in Figure 3. The large clusters are truncated by the finite size of the simulated system, resulting in the appearance of a hump of n_S at large S . Right at the percolation threshold, the cluster size distribution n_S follows the power law $n_S \sim S^{-\tau}$ in a widest range of cluster sizes in various aqueous systems.^{32,39} In the densely packed lysozyme powder, n_S follows a power law in the range of cluster sizes up to 200 molecules, when $N_w = 1000$ (see red circles in Figure 3). Oscillatory deviations from the power law behavior could not be eliminated by improving the statistics and should be attributed to the peculiar arrangement of the lysozyme molecules in the model powder. For large S to the left to the hump position, the distribution n_S deviates from the power law upward below the percolation threshold and downward above the percolation threshold.^{32,39} Hence, the cluster size distributions indicate a percolation threshold at $N_w \approx 1000$, corresponding to a water mass fraction $C \approx 0.17$, that is quite close to the threshold value $C_2(d_f) = 0.175$ estimated from the behavior of the fractal dimension d_f of the largest cluster (see Figure 1).

The formation of an infinite water network can also be explored by studying the evolution of the largest cluster from a nonspanning to a spanning structure. In addition to the fractal dimension, we also studied the size distribution of the largest cluster $P(S_{\text{max}})$ at various hydration levels. Usually, $P(S_{\text{max}})$ appears as an asymmetric curve with a maximum which becomes sharper with increasing system size. Distributions $P(S_{\text{max}})$ for the water in the densely packed protein powder at different hydration levels are shown in Figure 4. Close to the percolation threshold, $P(S_{\text{max}})$ shows obviously a two-peak structure at $T = 400$ K. A similar evolution of $P(S_{\text{max}})$ was observed for 2D lattices^{41,42} and for water at a planar hydrophilic surface.³⁹ It was found that the left peak represents finite largest clusters, while the right peak is due to infinite (spanning) clusters. When the spanning probability R is close to 50%, the

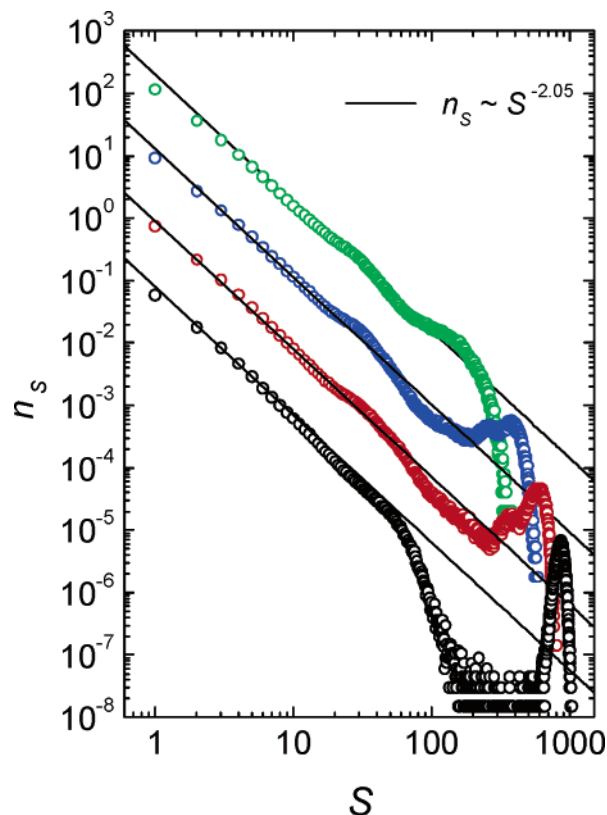


Figure 3. Probability distributions n_s of clusters with S water molecules in the densely packed powder at $T = 400$ K. The hydration level increases from $N_w = 700$ (top) to 1200 (bottom). Blue circles represent n_s at $N_w = 850$, when a spanning cluster exists with a probability of about 50%, while the red circles correspond to $N_w = 1000$, when the fractal dimension of the largest cluster is close to the 2D percolation threshold value. The distributions are shifted consecutively by 1 order of magnitude each, starting from the bottom.

two maxima in $P(S_{\max})$ have roughly the same height. The two-peak structure of $P(S_{\max})$ is pronounced in small systems and vanishes with increasing system size.

At lower temperature ($T = 300$ K), the two-peak structure of $P(S_{\max})$ is not so clear (Figure 4, left panel) due to the additional structure of the left peak. The splitting of the left peak of $P(S_{\max})$ could reflect the binding of the largest water clusters to some particular hydrophilic sites of lysozyme powder at low hydration levels.

The same cluster properties were studied for water in the loosely packed lysozyme powder model, described above. The course of the spanning probability R and the fractal dimension d_f of the largest cluster in loosely packed and densely packed powders with increasing hydration level are compared in Figure 5 at $T = 300$ K. In the loosely packed powder, the percolation transition of water is noticeably shifted to higher hydration levels. In particular, the threshold value $C_1(R) = 0.235 \pm 0.002$ in the loosely packed powder is almost twice the corresponding value $C_1(R) = 0.122 \pm 0.002$ in the densely packed powder. Similarly, the threshold value $C_2(d_f)$ is also essentially higher in the loosely packed powder (Figure 5, Table 1). The percolation threshold value, estimated from the cluster size distributions n_s in the loosely packed powder (not shown here), noticeably exceeds this value of $C_2(d_f)$. These observations, as well as the lowering of n_H at this threshold in comparison with the densely packed powder (Table 1), could mean that the spanning water network at the percolation threshold in loosely packed powder is not two-dimensional. Visual inspection of the simulation systems evidences that the spanning water network

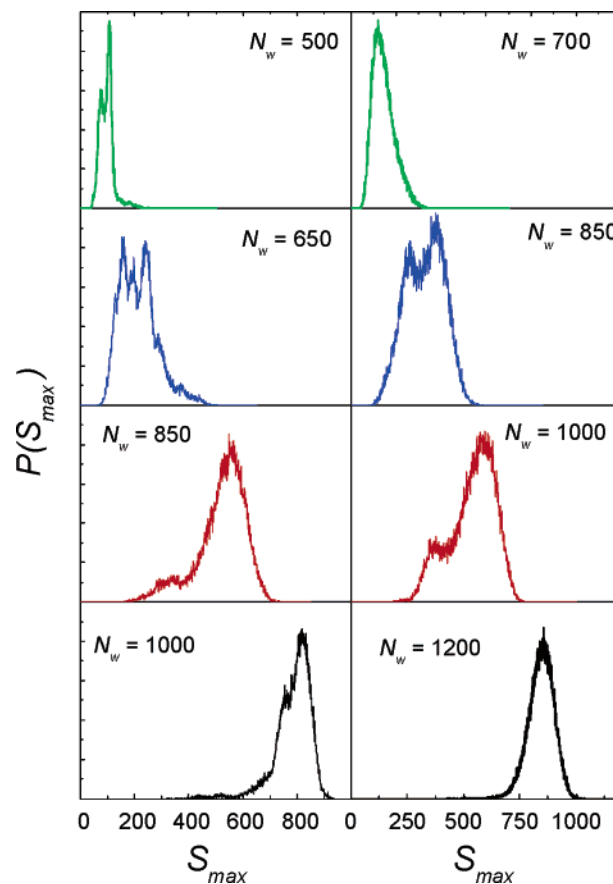


Figure 4. Probability distribution $P(S_{\max})$ for the largest cluster size S_{\max} of the water molecules in densely packed lysozyme powder at $T = 300$ K (left panel) and at $T = 400$ K (right panel) at various hydration levels. Green lines: below the percolation threshold; blue lines: R is about 50% ($C_1(R)$); red lines: 2D percolation threshold ($C_2(d_f)$); black lines: above the percolation threshold.

consists of 2D sheets at the protein surface as well as of 3D water domains, formed due to capillary condensation of water in hydrophilic cavities. The latter effect causes the essential distortion of various distribution functions of water clusters in the loosely packed powder.

Formation of a Spanning Water Network on Hydrophilic Spherical Surfaces. Infinite water clusters cannot appear on the surface of a finite object, such as a sphere or a single protein molecule. Strictly speaking, the probability R of finding an infinite cluster is equal to zero in such cases. Nevertheless, a transition from an ensemble of finite water clusters to a water network, which spans over the whole object, should be expected. To locate and characterize this specific percolation transition of water at the surface of hydrophilic spheres and single molecules, we have analyzed the cluster size distribution n_s , the mean cluster size S_{mean} , the fractal dimension d_f of the largest cluster, and its size distribution $P(S_{\max})$ at various levels of surface coverage C^* .

To detect and characterize the formation of a spanning network on the surface of a finite object, we determined threshold values of the surface coverage from various properties: the mean cluster size S_{mean} achieves a maximum at $C^*_{1}(S_{\text{mean}})$, the size distribution of the largest cluster $P(S_{\max})$ shows two peaks of comparable height at $C^*_{1}(S_{\max})$, and the fractal dimension d_f of the largest cluster achieves d_f^{2D} at $C^*_{2}(d_f)$. The obtained threshold values are shown in Table 2. The mean cluster size S_{mean} passes through the maximum practically at the same surface coverage, when the two peaks in $P(S_{\max})$

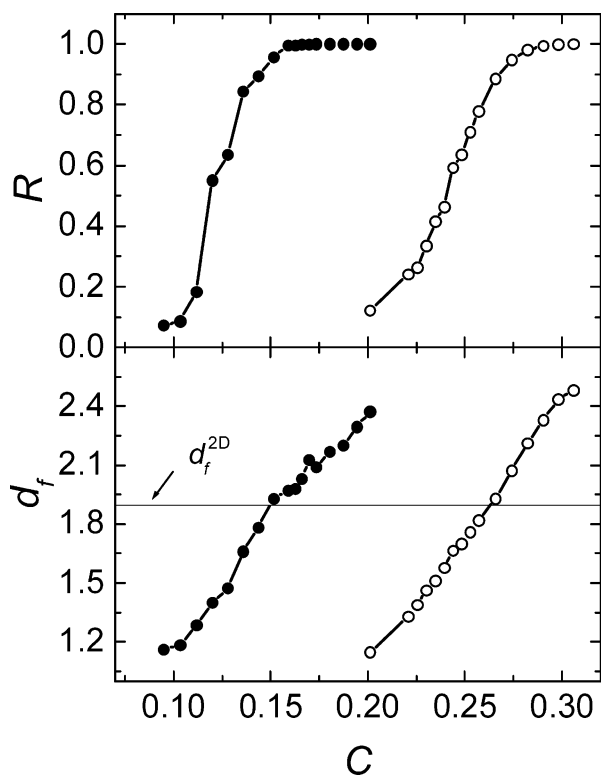


Figure 5. Spanning probability R (top) and fractal dimension d_f of the largest water cluster (bottom) as a function of the water mass fraction C in densely packed (solid circles) and loosely packed (open circles) powders at $T = 300$ K.

have similar heights, that is, $C^*_1(S_{\text{mean}}) \approx C^*_1(S_{\text{max}})$ for the three studied spheres and two temperatures (Table 2). They both approach the threshold value $C^*_2(d_f)$ with increasing sphere radius. The average number of hydrogen-bonds n_H at this surface coverage (Table 2) is close to the threshold values in 2D lattices²⁰ and lysozyme powder (Table 1).

The size distributions n_S of water clusters at the surface of a hydrophilic sphere for several hydration levels are shown in Figure 6. n_S shows the power law behavior in the widest range of cluster sizes at the surface coverage $C^*_2(d_f)$ (see Table 2). The two maxima of n_S , clearly seen at large S , are directly connected to the two-peak structure of the distribution of the largest cluster $P(S_{\text{max}})$.

In general, the growth of the water clusters with increasing hydration level is very similar at the surface of a finite object and in an infinite system (the lysozyme powder, considered above, or periodic planar hydrophilic surfaces³⁹). This similarity allows us to distinguish spanning and nonspanning water clusters on the surface of a finite object and to determine the minimum surface coverage, providing the permanent presence of a spanning network. Namely, a spanning cluster should belong to the right (large size) peak of the distribution $P(S_{\text{max}})$ of the largest cluster, and therefore it could be easily detected in the case of a pronounced two-peak structure of $P(S_{\text{max}})$. A spanning network starts to be permanently present when the fractal dimension of the largest cluster approximately achieves the value 1.896 expected at the 2D percolation threshold.

The changes of $P(S_{\text{max}})$ on the surfaces of two hydrophilic spheres with increasing water coverage is shown in Figure 7. The two-peak structure of $P(S_{\text{max}})$ is clearly seen in the considered range of surface coverage. It is evident that two maxima in $P(S_{\text{max}})$ have roughly the same height when the probability of finding a spanning cluster is close to 50%. At this hydration level, the two peaks are rather narrow at $T =$

425 K (blue lines in Figure 7). They become broader, but still distinct, at $T = 475$ K. Surprisingly, the two-peak structure of $P(S_{\text{max}})$ seems to be only weakly sensitive to the size of the sphere. Since the surface of a sphere should approach an infinite planar surface with increasing radius, one may expect the vanishing of the two-peak structure of $P(S_{\text{max}})$ with increasing sphere radius. To test this expectation, we performed simulations of the water clustering at the surface of a very large sphere (radius $R_{\text{sp}} = 50$ Å) with a surface area of more than 35 000 Å². The evolution of $P(S_{\text{max}})$ with increasing surface coverage at this spherical surface (Figure 8) is similar to the ones observed at the smaller spherical surfaces (Figure 7). Surprisingly, the two-peak structure of $P(S_{\text{max}})$ is still pronounced at the surface coverage $C^*_1(S_{\text{max}})$ (see Figure 9), which is close to $C^*_1(S_{\text{mean}})$, where the mean cluster size S_{mean} passes through the maximum (see Table 2).

The positions of the two peaks in the distribution $P(S_{\text{max}})$ give the most probable size of the largest nonspanning and spanning clusters. These positions could be estimated visually or determined from a fit of $P(S_{\text{max}})$. For example, $P(S_{\text{max}})$ could be fitted by a sum of Gaussians:

$$P(S_{\text{max}}) = \sum \frac{a_i}{w_i} \exp\left(-\frac{2(S_{\text{max}} - S_{\text{max},i})^2}{w_i^2}\right) \quad (2)$$

where $S_{\text{max},i}$, w_i , and a_i are position, half-width, and amplitude of the i th peak, respectively. It is not possible to fit perfectly the obtained distributions $P(S_{\text{max}})$ by two Gaussians, because the right side of the second peak falls sharply due to the truncation of the spanning cluster on the finite (spherical) surface. Neglecting the steep decay of $P(S_{\text{max}})$ to the right of the second peak and using two Gaussians in eq 2, we found that $S_{\text{max},2}$ is about twice $S_{\text{max},1}$ for all spheres studied. In Figure 9, we show such a fit of the distribution $P(S_{\text{max}})$ for the largest sphere, imposing $S_{\text{max},2} = 2S_{\text{max},1}$ (see Figure 9, dot-dashed line). The restriction $S_{\text{max},2} = 2S_{\text{max},1}$ also allows us to fit perfectly the complete distribution $P(S_{\text{max}})$ by three Gaussians (see Figure 9, red line). Summarizing, the most probable size of a spanning water cluster on a spherical surface is about twice that of the largest nonspanning cluster at any hydration level where both are observable. This observation has not yet been discussed in any percolation theory, but can be seen also in some previously published studies (refs 41, 42).

Formation of a Spanning Water Network on the Surface of a Single Lysozyme Molecule. Clustering of water on the surface of a single lysozyme molecule was analyzed along the lines employed to hydrophilic spherical surfaces. The fractal dimension d_f of the largest cluster achieves the value d_f^{2D} of the 2D percolation threshold approximately at the same surface coverage (Figure 10), when the cluster size distribution n_S obeys the power law in the largest range of cluster sizes (Figure 11, red circles). This gives the following estimations of the minimum water coverage, which enables the persistent existence of a spanning water network at the surface of the lysozyme molecule: $N_w = 450$ ($C^*_2(d_f) = 0.065$ Å⁻²) at $T = 300$ K and $N_w = 690$ ($C^*_2(d_f) = 0.100$ Å⁻²) at $T = 400$ K (Table 2).

The mean cluster size S_{mean} passes through a maximum at slightly lower hydration levels: $C^*_1(S_{\text{mean}}) = 0.056$ and 0.089 Å⁻² at $T = 300$ and 400 K, respectively (Figure 10, upper panel). The evolution of the distribution $P(S_{\text{max}})$ with the hydration level evidences a two-peak structure, which appears as two distinct maxima at $T = 300$ K, and which is still visible at $T = 400$ K (Figure 12). The behavior of $P(S_{\text{max}})$ indicates that the probability for the existence of a spanning water network is about

TABLE 2: Water Coverage C^* (in \AA^{-2}) on the Surface of a Single Lysozyme and on Hydrophilic Spheres^a

system	$C^*_1(S_{\max})$	$C^*_1(S_{\text{mean}})$	$C^*_{2}(d_f)$	$n_{\text{H}}(C^*_2)$	$N_w(C^*_2)$	$N_w^1(C^*_2)$
lysozyme, 300 K	0.058	0.056	0.065	2.26	450	336
lysozyme, 400 K	0.091	0.089	0.100	2.04	690	354
sphere $R_{\text{sp}} = 15 \text{ \AA}$, 425 K	0.086	0.082	0.096	2.11	390	350
sphere $R_{\text{sp}} = 30 \text{ \AA}$, 425 K	0.080	0.080	0.094	2.14	1270	1143
sphere $R_{\text{sp}} = 50 \text{ \AA}$, 425 K	0.087	0.087	0.092	2.15	3250	2925
sphere $R_{\text{sp}} = 15 \text{ \AA}$, 475 K	0.111	0.110	0.122	1.95	490	390

^a When: the mean cluster size S_{mean} passes through the maximum, $C^*_1(S_{\text{mean}})$, two peaks in $P(S_{\max})$ have the same height, $C^*_1(S_{\max})$, and d_f achieves the 2D threshold value $d_f^{2D} = 1.896$, $C^*_{2}(d_f)$. System properties at the surface coverage $C^*_{2}(d_f)$: $n_{\text{H}}(C^*_2)$, average number of hydrogen-bonds formed by each water molecule; $N_w(C^*_2)$, total number of water molecules; $N_w^1(C^*_2)$, number of water molecules in the first hydration shell.

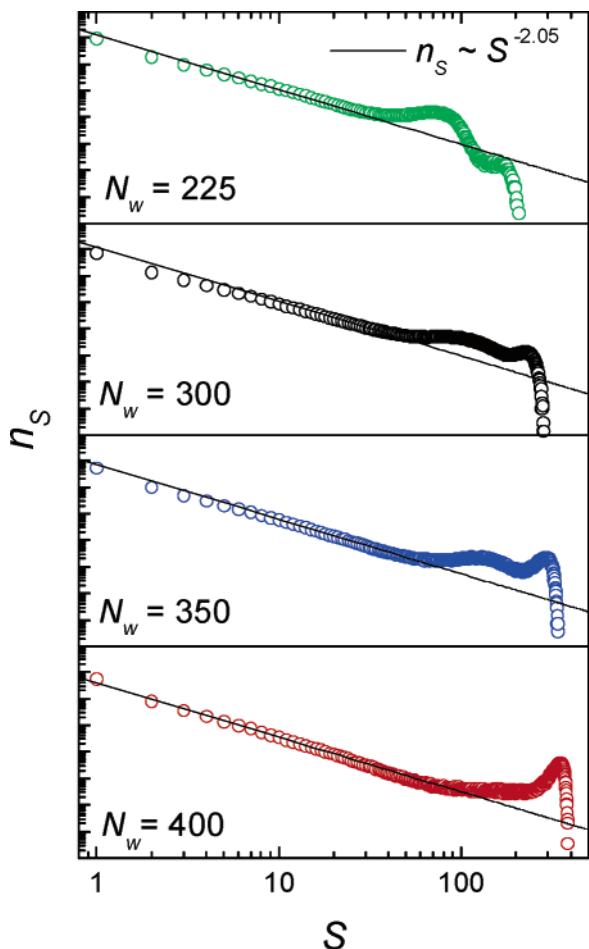


Figure 6. Probability distributions n_S of clusters with S water molecules at the surface of a hydrophilic sphere of radius $R_{\text{sp}} = 15 \text{ \AA}$ at $T = 425 \text{ K}$. The surface coverage increases from top to bottom. At $N_w = 350$, a spanning cluster exists with a probability of about 50%. At $N_w = 400$, the fractal dimension of the largest cluster is close to the 2D percolation threshold value.

50% when $N_w \approx 400$ ($C^*_1(S_{\max}) = 0.058 \text{ \AA}^{-2}$) at $T = 300 \text{ K}$ and $N_w \approx 625$ ($C^*_1(S_{\max}) = 0.091 \text{ \AA}^{-2}$) at $T = 400 \text{ K}$. The ratio of the most probable sizes of spanning $S_{\max,2}$ and nonspanning $S_{\max,1}$ largest clusters, estimated from the positions of the two peaks of $P(S_{\max})$, is about 1.6 for both temperatures. This value is smaller than the value ~ 2 obtained for spherical hydrophilic surfaces, probably due to the nonspherical shape of lysozyme and/or the inhomogeneous distribution of the hydrophilic sites on the protein surface.

When the two peaks of $P(S_{\max})$ have comparable heights, the surface water exists with equal probability in two quite different states: with spanning network and without it. Examples of these two kinds of water ordering scenarios are depicted in Figure 13. In the case of a spanning water network (Figure 13, upper part) the largest cluster envelopes the whole lysozyme molecule.

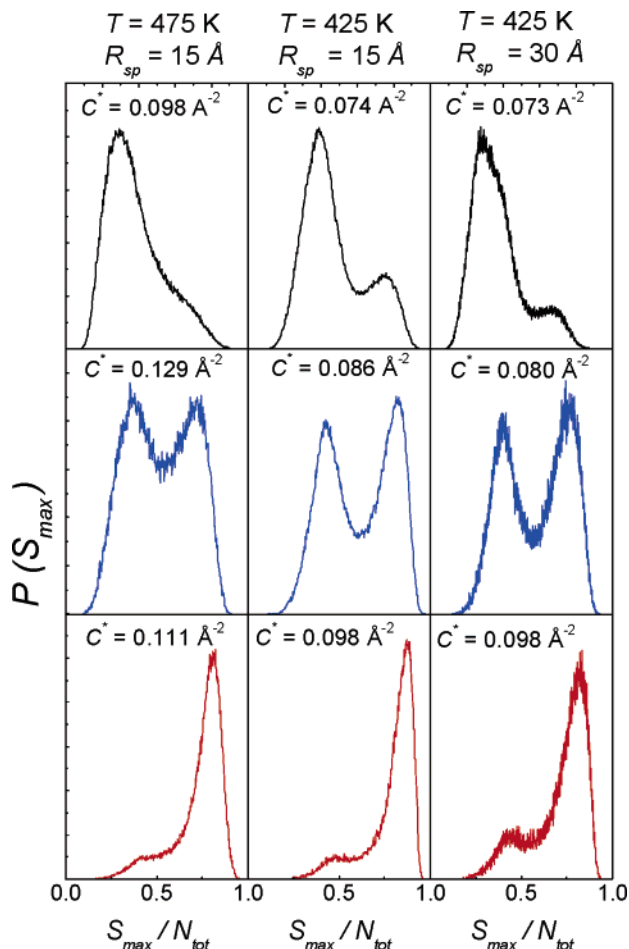


Figure 7. Probability distribution $P(S_{\max})$ of the size of the largest water cluster S_{\max} at the surfaces of hydrophilic spheres with the radii $R_{\text{sp}} = 15$ and 30 \AA at various hydration levels and temperatures. Upper panel: below the percolation threshold. Middle panel: the probability of a spanning cluster is about 50%. Lower panel: 2D percolation threshold.

The nonspanning largest water cluster is usually attached to some strongly hydrophilic part of the lysozyme (for example, to the left-bottom or to the cleft in the middle part of the molecule) (Figure 13, lower panel). Because of the large difference between $S_{\max,2}$ and $S_{\max,1}$, strong fluctuations of the water network occur at this surface coverage. Spanning and nonspanning structures of the surface water replace each other frequently. The lifetime of the distinct types of configurations is comparable to the lifetime of single water–water hydrogen-bonds ($\sim 0.2 \text{ ps}^{43}$).

It is interesting to compare the hydration levels, which provide the formation of a spanning water network at the surface of a single lysozyme molecule and in the model lysozyme powder. As an example, the course of the fractal dimension of the largest cluster d_f in the cases of the single lysozyme molecule and the

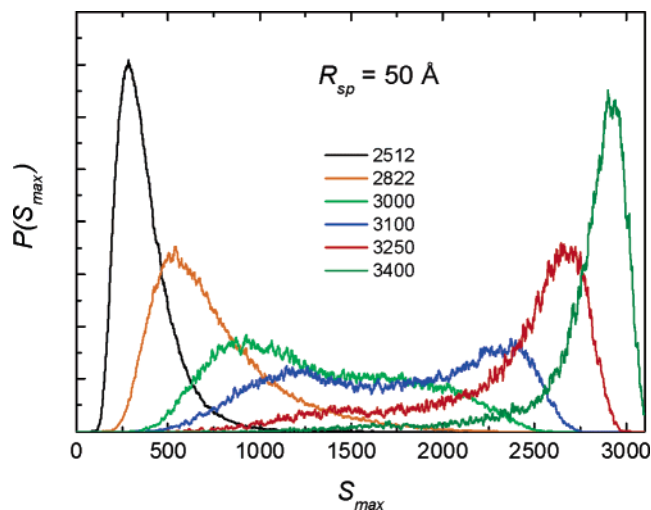


Figure 8. Probability distribution $P(S_{\max})$ of the largest water cluster at the surface of a hydrophilic sphere with radius $R_{\text{sp}} = 50 \text{ \AA}$ at $T = 425 \text{ K}$. The number of water molecules N_w are given in the legend. Blue line: probability of a spanning water cluster of about 50%. Red line: 2D percolation threshold.

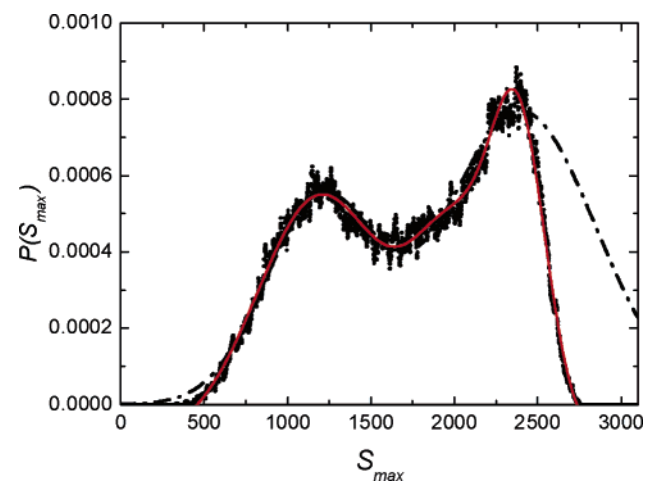


Figure 9. Probability distribution $P(S_{\max})$ of the largest water cluster at the surface of the hydrophilic sphere with radius $R_{\text{sp}} = 50 \text{ \AA}$ at $T = 425 \text{ K}$ and hydration level $N_w = 3100$ (symbols). The lines show fits to eq 2 (see text for details).

lysozyme powder are compared in the Figure 14. The threshold hydration level, expressed as mass fraction of water C , is essentially higher in the case of the single lysozyme molecule (Figure 14, left panel), because in the powder the accessible surface of the lysozyme molecules decreases due to their contacts and, additionally, the water molecules could simultaneously belong to the hydration shells of two or more lysozymes. Taking into account that the number of bonds per particle at the percolation threshold is rather universal and depends mainly on the system's dimensionality,²⁰ it is reasonable to consider the threshold hydration level in terms of the average number of water–water hydrogen-bonds n_H of the water molecule. The dependence of the fractal dimension of the largest cluster d_f on n_H , shown in Figure 14 (right panel), indicates a close coincidence of the 2D percolation thresholds in lysozyme powder and on the surface of a single lysozyme molecule. In particular, the spanning 2D water network appears in the two systems approximately at the same values of n_H at both studied temperatures (Tables 1 and 2). So, n_H could serve as a highly universal occupancy variable for such complex systems as hydrated proteins.

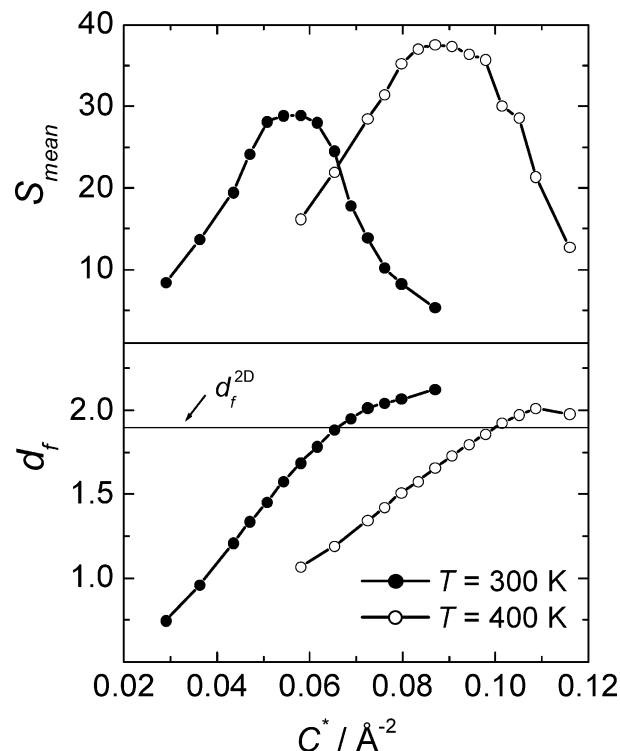


Figure 10. Mean cluster size S_{mean} (upper panel) and fractal dimension d_f of the largest water cluster (lower panel) on the surface of a single lysozyme molecule as a function of the surface coverage.

Discussion

An analysis of the water clustering in hydrated model lysozyme powder and on the surface of a single lysozyme molecule reveals the formation of a spanning water network with increasing hydration level via a percolation transition of the hydration water adsorbed on the protein surface, in agreement with experimental studies of protein powders.^{2,4–13} The fractal dimension of the largest water cluster d_f and the average number of hydrogen-bonds n_H at the percolation threshold (Figures 1, 5, 10, and 14) evidence the 2D character of the percolation transition, which was in fact established experimentally by determining the critical exponent of the protonic conductivity near the percolation threshold of water in powders of lysozyme,⁵ purple membrane,⁶ maize seeds,⁷ and yeast.¹³

The percolation threshold in a model of densely packed lysozyme powder at $T = 300 \text{ K}$ is found to be in good agreement with the experimental studies. The obtained mass fraction of water at the percolation transition $C_2(d_f) = 0.155$ (hydration level $h = 0.183$) is close to the experimental values for hydrated lysozyme powders $C = 0.132$ ($h = 0.152 \pm 0.016$).⁴ So, our rather crude model of densely packed lysozyme powder satisfactorily reproduces the clustering of water in real systems near the percolation threshold. Taking into account that in the artificial loosely packed model powder ($\rho = 0.44 \text{ g cm}^{-3}$) the percolation transition of water is distorted and strongly shifted toward higher water content, an improved model powder should have a density of the dry protein slightly above 0.66 g cm^{-3} of our dense powder model. Further improvement of the model should account for changes of the powder structure and density with the level of hydration. Finally, the powder should consist of flexible protein molecules. However, the current level of simulation technique and computer facilities make the application of the latter two improvements a major effort.

Our simulations allow a detailed exploration of the arrangement of the water molecules near hydrated proteins and its

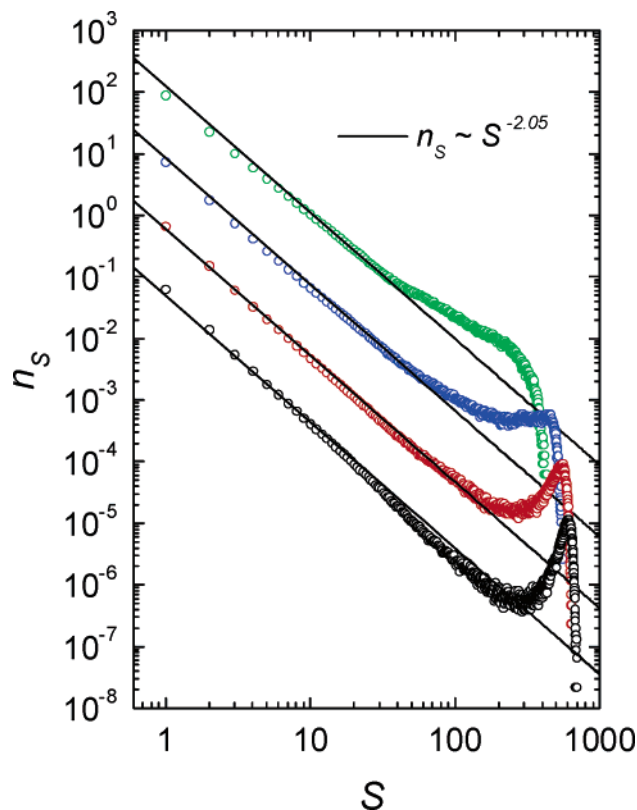


Figure 11. Distributions n_s of clusters with S water molecules at the surface of a single lysozyme molecule at $T = 400$ K. The surface coverage increases from $N_w = 525$ (top) to 750 (bottom). Blue circles: $N_w = 625$, a spanning network exists with a probability of about 50%. Red circles: $N_w = 700$, the fractal dimension d_f of the largest cluster is close to the 2D percolation threshold value. The distributions are shifted consecutively by 1 order of magnitude each, starting from the bottom.

changes during the percolation transition. Experimental studies⁴ provide only the average number of water molecules per one protein ($N_w/N_p \approx 120$) at the percolation threshold. However, this number may not correspond to the average number of water molecules N_w^1 in the first hydration shell of each protein in the powder. In our densely packed powder, $N_w/N_p \approx 146$ and $N_w^1 \approx 149$ at the percolation threshold at 300 K, indicating that most of the water molecules belong to a hydration shell which is not shared by several protein molecules. These numbers are significantly smaller than $N_w = 450$ and $N_w^1 \approx 336$ for the percolation threshold at the surface of a single lysozyme molecule at the same temperature (Table 2). Such a strong difference can be attributed to a significant decrease of the accessible surface area of proteins in the powder due to close contacts. So, the 2D percolation transition of water in protein powder appears as the formation of a water network, which spans the extended “collective” surface created by close-packed protein molecules, covering each protein molecule only partially.

Our crude model of a protein powder does not change its structure with the level of hydration, and therefore it is not reliable at high hydration levels. Nevertheless, we can make some predictions on the basis of our simulations of a single hydrated protein molecule. In particular, at the percolation threshold in the powder ($h = 0.183$), about 190 molecules per protein molecule are missing to form a spanning network around each protein. This could be achieved at $h \sim 0.30$, if all excess waters above the threshold hydration are shared by two proteins. Finally, the formation of separate spanning networks could be expected at $h \approx 0.42$.

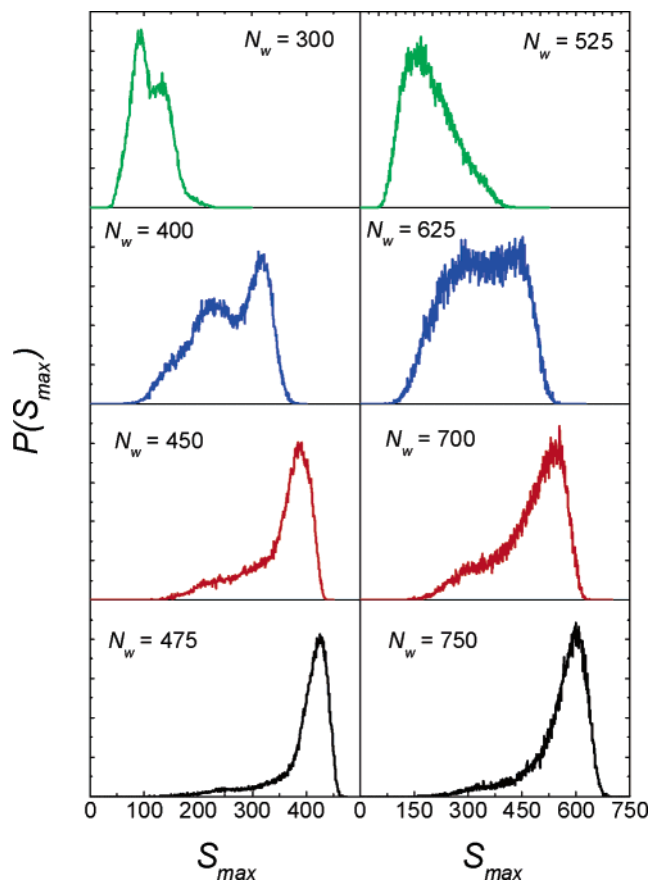


Figure 12. Probability distribution $P(S_{\max})$ of the largest water cluster S_{\max} on the surface of a single lysozyme molecule at $T = 300$ K (left panel) and 400 K (right panel) and various hydration levels. Green lines: below the percolation threshold; blue lines: probability of a spanning cluster is about 50%; red lines: 2D percolation threshold; black lines: above the percolation threshold.

The analysis of the experimental data^{2,12} indicated three important hydration levels of lysozyme: the 2D percolation threshold is observed at $h \approx 0.152$; the water motion increases strongly at $h \approx 0.25$; and the full internal motions of the protein recover at $h \approx 0.38$. Dividing the characteristic values of h estimated above from the simulations by a factor of about 1.15, we obtain a surprising coincidence with these experimentally observed specific hydration levels. The factor 1.15 is equal to the ratio of SASA of our model lysozyme (6900 \AA^2) and SASA calculated from the crystal structure (6000 \AA^2).² This seems to be the main origin of the differences between the hydration levels estimated from experiment and computer simulations. The close similarity of the protein hydration in experiments and simulations shows that an individual (nonshared) spanning water network around the protein molecule is a necessary condition for its full internal motions. The formation of a fractal-like spanning network on a protein molecule via a 2D percolation transition reflects the first appearance of an individual hydration shell.

It is interesting to estimate which part of the lysozyme surface is covered by water at the percolation threshold. A water monolayer with bulklike structure (corresponding to a density of about 0.033 \AA^{-3} at ambient conditions) gives a surface coverage of about 0.1 \AA^{-2} . This coverage does not change strongly due to packing effects near planar smooth surfaces¹⁹ or near model protein surfaces,^{30,44} and therefore, 10 \AA^2 could be used as an average area occupied by a water molecule at the surface. At the percolation threshold on the surface of a single lysozyme at $T = 300$ K, water covers about 50% of the total

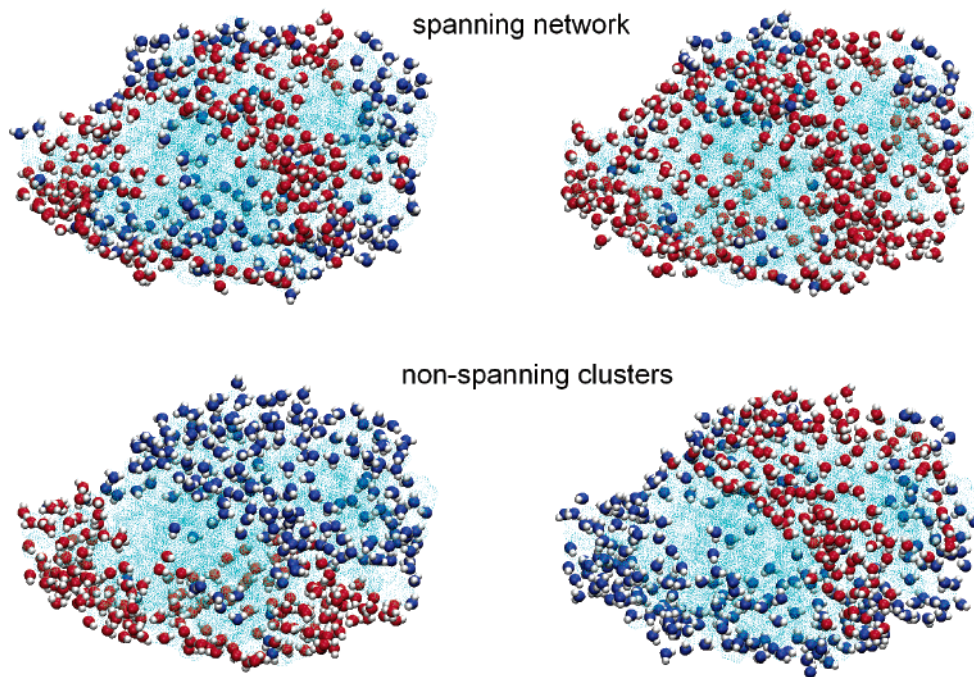


Figure 13. Arrangement of water molecules on the surface of a lysozyme molecule at the hydration level, where the probability of finding a spanning water network is about 50% ($T = 300$ K, $N_w = 400$). The oxygen atoms of the water molecules which belong to the largest cluster are colored in red, those of all other water molecules in blue. Examples of spanning and nonspanning water clusters are shown in the upper panel and lower panel, respectively.

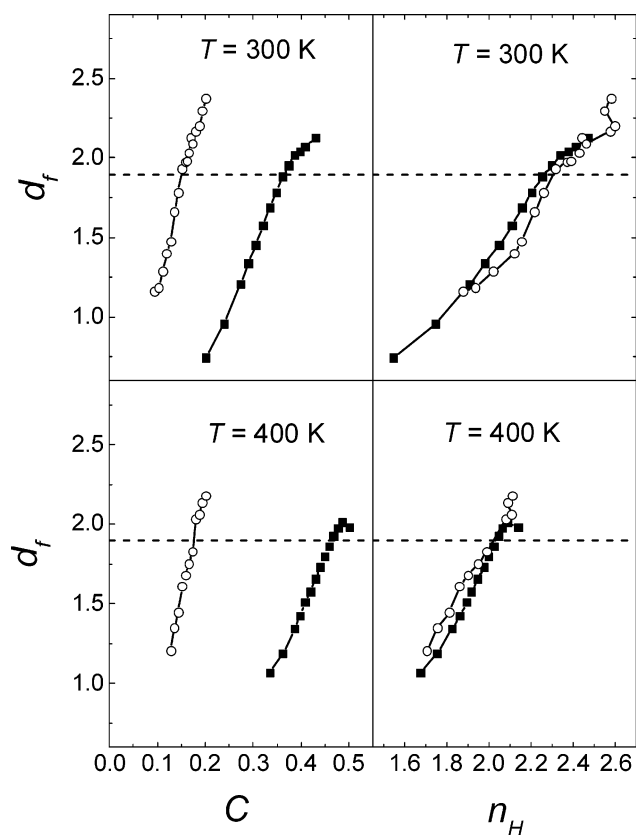


Figure 14. Fractal dimension of the largest water clusters as a function of the water mass fraction (left panel) and as a function of the average number of hydrogen-bonds n_H (right panel): single lysozyme (solid squares) and densely packed powder (open circles) at $T = 300$ and 400 K. Dashed lines: $d_f^{2D} = 1.896$.

lysozyme surface, or about 66% of the hydrophilic part of the lysozyme surface. (We estimate that about 74% of the lysozyme surface is hydrophilic, considering polar and charged residues.)

The value 66% is close to the site occupancy at the percolation threshold of square and honeycomb 2D lattices, which consists of sites with 4 and 3 nearest neighbors, respectively. The above-mentioned surface occupancy should not be mixed up with the so-called space occupation probability, which is 0.45 ± 0.03 at the 2D site percolation threshold regardless of the lattice structure.⁴⁵ The latter parameter was used in the analysis of water percolation at protein surfaces.^{2,4-7,12} Note, that the space occupation probability uses a specific normalization to the whole surface area instead of the conventional normalization to the complete coverage, defined as the maximum packing of particles. Neglecting this difference gives diverse nonuniversal critical values for the space occupation probability.^{2,4,6,7}

There are several experimental estimates of the water coverage at the percolation threshold in protein systems. They were determined as the ratio of the hydration level h_c at the percolation threshold and at some higher hydration level h_m , which was attributed to the monolayer coverage. The value h_c/h_m as well as h_c and h_m vary strongly from system to system. In lysozyme powder, $h_c/h_m = 0.40^4$ (to be compared with the value 0.42 from our simulations, see above), in purple membrane $h_c/h_m = 0.18$,⁶ and in embryo and endosperm of maize seeds h_c/h_m values are 0.36 and 0.70, respectively.⁷ Our simulations indicate that h_m is close to the threshold coverage of a single molecule, and, therefore it should depend mainly on protein hydrophilicity. The value h_c depends on the hydrophilicity of the protein molecules, topological features of its surface, and packing of molecules in powder. Therefore, experimentally observed strong variations of the ratio h_c/h_m reflect mainly the peculiarity of protein packing.

At $T = 300$ K, about 75% of the water molecules belong to the first hydration shell of a single lysozyme molecule at the percolation threshold, and this fraction noticeably decreases with further increase of the hydration level. For comparison, in the case of hydrophilic spheres, this value is about 90% at $T = 425$ K. This evidences that the lysozyme surface is noticeably

less hydrophilic than the studied smooth hydrophilic surface, which approximately corresponds to the minimum hydrophilicity necessary for the occurrence of a layering transition (2D condensation).¹⁹ So, a layering transition cannot be expected on a lysozyme surface.

Finally, we discuss the perspectives of computer simulations of water percolation in hydrated protein systems. More realistic powder models with flexible molecules should be used to clarify the role of protonic conductivity and protein dynamics at the onset of protein function. It seems useful to explore first the dynamic properties of a single protein as well as its structure at hydration levels on both sides of the percolation threshold of the surface water. Besides, the influence of the large fluctuations of the water network close to the percolation threshold on the properties of the hydrated protein should be clarified. In addition, studying the spanning water network around protein molecules in aqueous solutions and its breakage by temperature or cosolvents could also be useful for the understanding of the protein behavior in complex solutions. Our preliminary results⁴⁶ show that the clustering of the water molecules near the flexible protein and peptide molecules in infinitely diluted aqueous solution is similar to that presented above for a low-hydrated single lysozyme molecule.

Percolation transitions in closed system, such as the surface of a finite object, have physical significance not only for the processes in the hydration shells of proteins but also for relaxation processes in glasses.⁴⁷ This percolation problem did not attract much attention till now, but definitely deserves further studies in the framework of a percolation analysis. In particular, various properties of spanning and nonspanning networks as well as appropriate criteria to detect spanning networks in simulations should be studied systematically.

Acknowledgment. We thank J. Kertesz and D. Stauffer for discussions concerning the percolation analysis and the Deutsche Forschungsgemeinschaft (DFG-Forschergruppe 436) for financial support. We are also indebted to the referees for useful comments.

References and Notes

- (1) Kuntz, I. D., Jr; Kauzmann, W. *Adv. Protein Chem.* **1974**, *28*, 239.
- (2) Rupley, J. A.; Careri, G. *Adv. Protein Chem.* **1991**, *41*, 37.
- (3) Pal, S. K.; Zewail, A. H. *Chem. Rev.* **2004**, *104*, 2099.
- (4) Careri, G.; Giansanti, A.; Rupley, J. A. *Proc. Natl. Acad. Sci. U.S.A.* **1986**, *83*, 6810.
- (5) Careri, G.; Giansanti, A.; Rupley, J. A. *Phys. Rev. A* **1988**, *37*, 2703.
- (6) Rupley, J. A.; Siemankowski, L.; Careri, G.; Bruni, F. *Proc. Natl. Acad. Sci. U.S.A.* **1988**, *85*, 9022.
- (7) Bruni, F.; Careri, G.; Leopold, A. C. *Phys. Rev. A* **1989**, *40*, 2803.
- (8) Pissis, P.; Anagnostopoulou-Konsta, A. *J. Phys. D: Appl. Phys.* **1990**, *23*, 932.
- (9) Klammler, F.; Kimich, R. *Croat. Chem. Acta* **1992**, *65*, 455.
- (10) Konsta, A. A.; Laudat, J.; Pissis, P. *Solid State Ionics* **1997**, *97*, 97.
- (11) Careri, G. *Prog. Biophys. Mol. Biol.* **1998**, *70*, 223.
- (12) Careri, G.; Peyrard, M. *Cell. Mol. Biol.* **2001**, *47*, 745.
- (13) Sokolowska, D.; Krol-Otwinowska, A.; Moscicki, J. K. *Phys. Rev. E* **2004**, *70*, 052901.
- (14) Careri, G.; Milotti, E. *Phys. Rev. E* **2003**, *67*, 051923.
- (15) Smith, J. C.; Merzel, F.; Bondar, A.-N.; Tournier, A.; Fischer, S. *Philos. Trans. R. Soc. London, Ser. B* **2004**, *359*, 1181.
- (16) Steinbach, P. J.; Brooks, B. R. *Proc. Natl. Acad. Sci. U.S.A.* **1993**, *90*, 9135.
- (17) Bizzarri, A. R.; Wang, C. X.; Chen, W. Z.; Cannistraro, S. *Chem. Phys.* **1995**, *201*, 463.
- (18) Tarek, M.; Tobias, D. J. *J. Am. Chem. Soc.* **1999**, *121*, 9740; *Biophys. J.* **2000**, *79*, 3244.
- (19) Brovchenko, I.; Geiger, A.; Oleinikova, A. *J. Chem. Phys.* **2004**, *120*, 1958.
- (20) Stauffer, D. *Introduction to Percolation Theory*; Taylor & Francis: London and Philadelphia, 1985.
- (21) McKenzie, H. A.; White, F. H., Jr. *Adv. Protein Chem.* **1991**, *41*, 174.
- (22) Berman, H. M.; Westbrook, J.; Feng, Z.; Gilliland, G.; Bhat, T. N.; Weissig, H.; Shindyalov, I. N.; Bourne, P. E. *Nucleic Acids Res.* **2000**, *28*, 235.
- (23) Kundrot, C. E.; Richards, F. M. *J. Mol. Biol.* **1987**, *193*, 157.
- (24) Cornell, W. D.; Cieplak, P.; Bayly, C. I.; Gould, I. R.; Merz, K. M., Jr.; Ferguson, D. M.; Spellmeyer, D. C.; Fox, T.; Caldwell, J. W.; Kollman, P. A. *J. Am. Chem. Soc.* **1995**, *117*, 5179.
- (25) Jorgensen, W. L.; Chandrasekhar, J.; Madura, J. D.; Impey, R. W.; Klein, M. L. *J. Chem. Phys.* **1982**, *77*, 926.
- (26) Berendsen, H. J. C.; Postma, J. P. M.; van Gunsteren, W. F.; DiNola, A.; Haak, J. R. *J. Chem. Phys.* **1984**, *81*, 3684.
- (27) Essmann, U.; Perera, L.; Berkowitz, M. L.; Darden, T.; Lee, H.; Pedersen, L. G. *J. Chem. Phys.* **1995**, *103*, 8577.
- (28) Kodandapan, R.; Suresh, C. G.; Vijayan, M. *J. Biol. Chem.* **1990**, *265*, 16126.
- (29) Kocherbirov, V.; Arnebrant, T.; Söderman, O. *J. Phys. Chem. B* **2004**, *108*, 19036.
- (30) Smolin, N.; Winter, R. *J. Phys. Chem. B* **2004**, *108*, 15928.
- (31) Geiger, A.; Stillinger, F. H.; Rahman, A. *J. Chem. Phys.* **1979**, *70*, 4185.
- (32) Oleinikova, A.; Brovchenko, I.; Geiger, A.; Guillot, B. *J. Chem. Phys.* **2002**, *117*, 3296.
- (33) Brovchenko, I.; Geiger, A.; Oleinikova, A. *Phys. Chem. Chem. Phys.* **2004**, *6*, 1982.
- (34) Jan, N. *Physica A* **1999**, *266*, 72.
- (35) Hovi, J.-P.; Aharony, A. *Phys. Rev. E* **1996**, *53*, 235.
- (36) Newman, M. E. J.; Ziff, R. M. *Phys. Rev. Lett.* **2000**, *85*, 4104.
- (37) Martins, P. H. L.; Plascak, J. A. *Phys. Rev. E* **2003**, *67*, 046119.
- (38) de Oliveira, P. M. C.; Nobrega, R. A.; Stauffer, D. *J. Phys. A: Math. Gen.* **2004**, *37*, 3743.
- (39) Brovchenko, I.; Oleinikova, A. In *Handbook of Theoretical and Computational Nanotechnology*; Rieth, M., Schommers, W., Eds.; American Scientific Publishers, 2005.
- (40) Brovchenko, I.; Geiger, A.; Oleinikova, A. In *New Kinds of Phase Transitions: Transformations in Disordered Substances*; Brazhshkin, V. V., Buldyrev, S. V., Ryshov, V. N., Stanley, H. E., Eds.; Kluwer Academic Publishers: Norwell, MA, 2002; p 367.
- (41) Sen, P. *J. Phys. A: Math. Gen.* **2001**, *34*, 8477.
- (42) da Silva, C. R.; Lyra, M. L.; Viswanathan, G. M. *Phys. Rev. E* **2002**, *66*, 056107.
- (43) Geiger, A.; Mausbach, P.; Schnitker, J.; Blumberg, R. L.; Stanley, H. E. *J. Phys. (Paris)* **1984**, *45*, C7-13.
- (44) Merzel, F.; Smith, J. C. *Proc. Natl. Acad. Sci. U.S.A.* **2002**, *99*, 5378.
- (45) Zallen, R.; Scher, H. *Phys. Rev. B* **1971**, *4*, 4471.
- (46) Brovchenko, I., et al. To be published.
- (47) Campbell, I. A.; Flesselles, J.-M.; Jullien, R.; Botet, R. *Phys. Rev. B* **1988**, *37*, 3825.